Evaluation of Saudi pegmatite and its use in porcelain industry

Hassan M.H. Al-Marzouki[1], Christopher Jeffery[2], Gamal A. Khater[3,*]

[1]*Saudi Geological Survey, Jeddah, Saudi Arabia*
[2]*University of Leicester, Geology Department, Leicester, United Kingdom*
[3]*National Research Center, Glass Research Dept., Dokki, Cairo, Egypt*

Received 14 April 2012; received in revised form 5 June 2012; accepted 10 July 2012

Abstract

Pegmatite is the main source of feldspar for ceramics industry. Usage of pegmatite in ceramic industry causes some problems due to the presence of mica and iron oxides. These materials reduce tile strength, hardness and density of the final product leading to low quality ceramic products. Southern Saudi pegmatite separation treatment was carried out in two phases in order to improve the ceramic quality of the feldspar obtained from this pegmatite. The first phase consists of gravitational separation to remove the heavy impurities and in the second phase magnetic separation was carried out to further minimize iron content. Porcelain ceramic batches were prepared by wet-mixing, drying, pressing (semi-dry press) and fired at temperatures from 1000 to 1350 °C. The porcelain ceramic bodies were prepared and examined by DTA, X-ray diffraction, SEM and tested for bulk density, linear shrinkage, water absorption and flexural strength. These results indicated that, after treatment (gravity and magnetic separation), the pegmatite can be considered as a good source of potash feldspar. The present study provides a positive indication for using of Southern Saudi pegmatite after treatment in ceramic industries.

Keywords*: traditional ceramics,synthesis and processing, porcelain, pegmatite*

I. Introduction

Alkali feldspars are one of the basic raw materials of ceramic and porcelain industries. Feldspars are alumina silicates containing K, Na and a small amount of Ca. They occur in different types of rocks such as granite, syenite and pegmatite. In fact, high-grade feldspar products are extracted from pegmatite deposits. In recent years the consumption of feldspar has been increased significantly together with the developing and changing technology. As pegmatite occurs in very limited quantities and very restricted geologic environment and does not meet the increasing demands there is a need to look for other rocks as potential reserve for feldspars. A majority of these rocks contain low-quality feldspar and undesirable impurities for ceramic and glass industries. Pegmatite consists of an important proportion of feldspar and quartz. Other minerals associated with these minerals are biotite muscovite and iron oxides. Generally, these minerals have specific magnetic properties and high density. Therefore it is possible to remove them in appropriate size.

Feldspars are commercially used in the glass and ceramics industries because of their chemical composition, particularly for their alkali content. The consumption of feldspars within these two industries is estimated at 85–90 % of the market [1]. Feldspar is also used in fillers and abrasive industries but not as much as in the ceramic and glass industries.

The greatest consumption of feldspar raw materials is in ceramic products. Ceramic products comprise sanitary ware, ceramic tiles, dinnerware, ceramic glazes, and electrical porcelain. In ceramic industries feldspar is a basic component in the raw material batch for ceramic bodies. The typical feldspar content in floor and wall tiles is from 10–55 wt.%, from 15–30 wt.% in white ware, chemical porcelain and hotel china, 25–35 wt.% in sanitary ware and 30–50 wt.% in electrical porcelain [2]. Feldspar is also used in ceramic glazing in amounts ranging from 30–50 wt.%; by providing alumina and alkali it

* Corresponding author: tel: +966 505486245
fax: +966 12650597, e-mail: *gamal.kh@saudiceramics.com*

also acts as a flux in fine ceramics [3]. In addition, feldspar also has various significant usages such as for ceramic shields. The NASA space programme has used a ceramic thermal shield to protect spacecraft during the re-entry to the atmosphere. In pottery, a high amount of potash feldspar increases their strength. Potash feldspar is also involved in the ceramic materials which increase the efficiency of gas turbines. A particular application that consumes a significant amount of feldspar is porcelain industry, which uses 60–80 %.

Fluxes are raw materials with high amount of alkaline oxides, mainly K_2O and Na_2O, whereby, in reaction with silica and alumina, promote liquid phase formation that facilitates the densification. The liquid phase surrounds the solid particles and by surface tension enables rearrangement of particles and decreasing the porosity [4–7].

Traditionally, porcelain is defined as a glazed or unglazed vitreous ceramic white ware, and is used also for technical purposes, such as electrical, chemical, mechanical, structural and thermal wares when they are vitreous.

Triaxial porcelain is primarily composed of clay, feldspar and a filler material (usually quartz or alumina). However, alumina can be substituted for quartz to increase the mechanical strength of the fired ware and sometimes nepheline syenite also can be substituted for feldspar. On thermal treatment, the triaxial porcelain system forms a mixture of glass and crystalline phases depending on the chemistry of the raw materials and processing type. The K_2O-Al_2O_3-SiO_2 and Na_2O-Al_2O_3-SiO_2 ternary phase diagrams provide useful information about the compositions of various types of industrial porcelains [5,8]. The phase transformation and microstructure of traditional triaxial porcelain (kaolinite-quartz-feldspar) bodies have been studied in great detail by many authors [9–12].

Generally, these types of porcelain are heterogeneous with crystalline phases (mainly quartz and mullite) and close spherical pores (in case of presence of a little porosity) dispersed in a glassy matrix. The chemical reactions involved in a porcelain body at various stages of thermal treatment have been discussed thoroughly [13–15]. Kaolinitic clay ($Al_2O_3 \cdot 2SiO_2 \cdot 2H_2O$) is the major raw material of a porcelain system (clay-quartz-feldspar), which undergoes dehydroxylation at around 550 °C and forms metakaolin ($Al_2O_3 \cdot 2SiO_2$). This is an endothermic process as detected in differential thermal analysis. Then, when the temperature ranges between 950 and 1000 °C, metakaolin decomposes into non-equilibrium spinel-type phases with the release of amorphous silica. At this temperature range feldspar reacts with silica and forms an eutectic. The exact eutectic temperature depends on the type of feldspar (potash or soda). Beyond 1000 °C, densification starts by a viscous flow sintering process followed by transformation of spinel phases to mullite ($3Al_2O_3 \cdot 2SiO_2$). The spinel is transformed into primary mullite and silica at temperatures above 1100 °C. Due to this reaction series, primary mullite is commonly observed in porcelain microstructure as an aggregate of small crystals (<0.5 mm) in the clay relicts. Secondary mullite is formed by the reaction of clay relicts with feldspar at around 1200 °C, and appears as a long needle crystal (>1 mm) [16].

The aim of this study is to evaluate and improve a Southern Saudi pegmatite as a source of feldspar for ceramic industry, to meet the increasing demands for other rocks as potential reserve for feldspars.

II. Experimental

2.1 Magnetic separation

Magnetic separation (MS) is the method carried out after gravity separation to separate the undesired materials which have magnetic properties. In the magnetic separation method only two size fractions are used namely 0.6–0.4 mm and 0.4–0.1 mm. The size fraction of 1.2–0.6 mm is disregarded because the presence of the iron oxide and mica are compacted with the light minerals hence the machine cannot separate them. In this work Jones high-intensity paramagnetic separator 1300 × 80 A/M was used.

Flotation experiments were conducted with –200 and –100 mm test samples in a self-aerated laboratory flotation cell. Conditioning time was kept constant at 5 min for rougher circuit and 3 min for cleaning circuits. Potassium oleate (100 g/t) was added in four steps at natural pH of 7.6. Pine oil was used as frothier in the first stage and in subsequent stages.

2.2 Porcelain ceramic compositions and batch preparation

In the present study, two ceramic compositions were selected designated as C1 (containing Southern Saudi pegmatite before magnetic separation) and C2 (containing Southern Saudi pegmatite after magnetic separation), keeping the content of other raw materials constant. Table 1 lists the compositions of the used natural raw materials. The details of ceramic compositions in oxide percentages and percentages of raw materials are given in Tables 2 and 3.

One kilogram from each raw material was weighed to be used in preparation of the batch compositions of the studied porcelain bodies (Table 3). Each batch was wet-ground in a pot mill for 18–20 h until the residue on a 200 mesh BS sieve was reduced to less than 1.5 wt.%. The produced specimens were dried, then powdered and classified into rectangular samples of dimensions 66 mm × 15 mm × 4 mm and cylindrical samples 25 mm in length using a hydraulically operated compacting press. A specific pressure of 450–500 kg/cm^2 was applied similar to the conditions in industry. In addition, the pressed samples were oven-dried until the moisture content was reduced to less than 0.5%. The dried cylindrical samples were thermally heated in a high temper-

Table 1. Chemical analyses of the raw materials used

Oxides	Raw materials [wt.%]			
	Pegmatite before MS	Pegmatite after MS	Clay	Quartz
SiO_2	71.80	72.32	45.41	98.66
Al_2O_3	14.59	14.99	34.39	0.39
Fe_2O_3	1.00	0.05	1.13	0.07
TiO_2	0.11	0.04	0.89	0.01
CaO	0.06	0.05	1.07	0.10
MgO	0.10	0.08	0.76	0.02
K_2O	10.00	9.10	0.42	0.12
Na_2O	2.00	3.18	0.87	0.09
L.O.I.	0.58	0.20	14.67	0.37

Table 2. Chemical composition of the porcelain bodies studied

Oxides	Chemical composition [wt.%]	
	C1	C2
SiO_2	62.83	62.86
Al_2O_3	28.64	28.65
Fe_2O_3	0.92	0.51
TiO_2	0.73	0.39
CaO	1.07	1.03
MgO	0.60	0.60
K_2O	3.78	3.42
Na_2O	1.10	2.58

Table 3. Batch composition of the porcelain bodies studied

Raw materials	Batch composition [wt.%]	
	C1	C2
Clay (kaolin)	60	60
Pegmatite before MS	30	Nil
Pegmatite after MS	Nil	30
Quartz	10	10

ature dilatometer furnace at a rate of 10 °C/min to study their densification behaviour.

Rectangular samples were heated in the temperature range of 1160–1200 °C in an electric furnace at the rate of 18 °C/min for period of 45 min at the peak temperature. The heated samples were tested for bulk density (BD), linear shrinkage, water absorption (WA%), and flexural strength (Instron 5500R).

2.3 Sample characterization

Differential thermal analysis and thermo gravimetric analysis (DTA-TGA) were carried out on Netzsch STA-490 using 60 mg of powdered samples, of grain size 0.2–0.6 mm heated alongside with Al_2O_3 powder as a reference material. A heating rate of 10 °C/min was maintained for all the runs.

Identification of crystals precipitating in the course of crystallization was conducted by the X-ray diffraction analysis of the powdered samples. The X-ray diffraction patterns were obtained using a Schimadzue XRD-600, Japan, adopting Ni-filtered CuKα radiation.

The microstructures of the samples were examined using a Hitachi S-3600N scanning electron microscope (SEM) operated under high vacuum conditions. The mineralogical constitutions were studied using Carl Zeiss polarizing microscope.

The electron microprobe (EMP) analytical procedure (developed at the Department of Geology, University of Leicester) were used to identify different minerals using wavelength dispersion on electron microprobe operating at 15 kV and 30 nA with a beam diameter of 10 μm. Approximately, 200 points were analyzed to identify different minerals such as quartz, mica and the feldspar end members.

The brightness and colour values were determined using a Hunter Lab. spectrocolourimeter. Values were compared to standard white reference body.

III. Results and discussion

X-ray diffraction analysis (Fig. 1) of Southern Saudi pegmatite after treatment (gravity and magnetic separation) showed that the selected four samples composed of K-feldspar (microcline, ASTM card No.12-703) as the major phase with a little amounts of quartz (ASTM card No.11-252) and albite (ASTM card No. 20-554). These results indicate that the pegmatite after this kind of treatment can be considered as a good source of potash feldspar.

The visual and optical microscopic examination of selected samples indicated that the Sothern Saudi pegmatite is essentially composed of K-feldspars (microcline) with low amounts of quartz and albite (Fig. 2). Microcline is characterized by a combination of albite and pericline twinning, while albite shows a polysynthetic twinning. Most microclines are microperthitic and retain the morphology of the monoclinic feldspar from which they have obtained. Microcline is characterized by cross-hatched texture. This is clear in Fig. 2a,b and confirmed literature results [17].

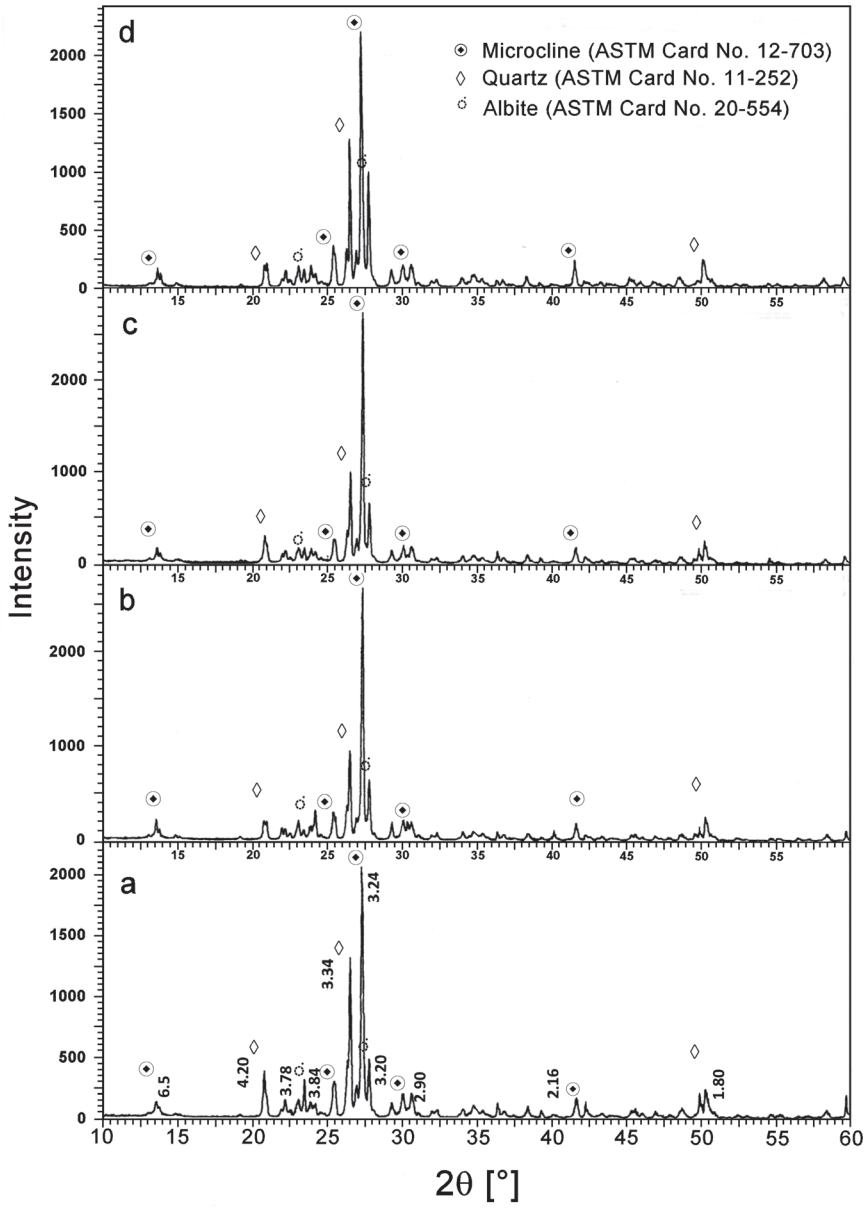

Figure 1. X-ray diffraction analyses of the selected four samples from Southern Saudi pegmatite

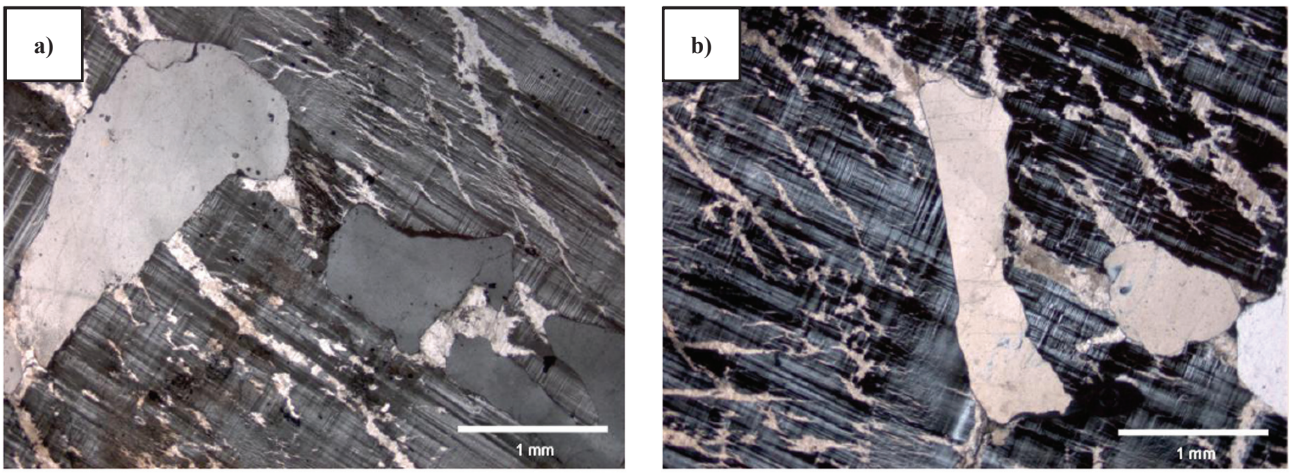

Figure 2. Photomicrographs of the investigated samples from Southern Saudi pegmatite: a) the microcline shows cross hatched, euhedral crystals of quartz and albite, and b) the intergrowth microcline with albite and prismatic crystals of quartz

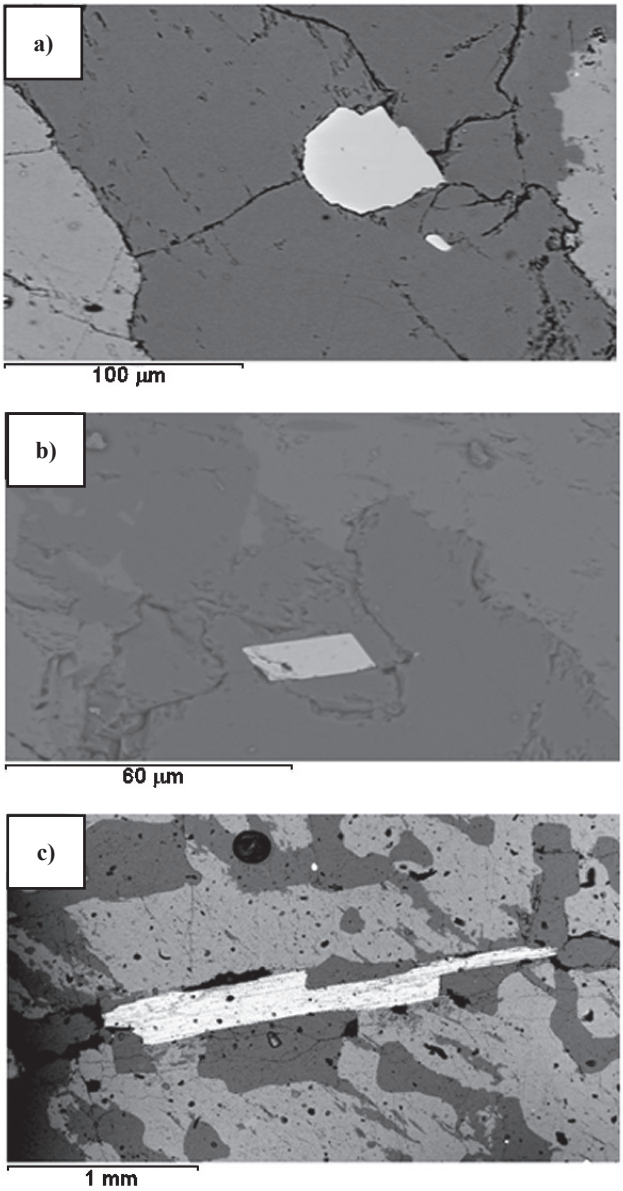

Figure 3. SEM backscattered images for feldspar impurities: a,b) magnetite crystals contact with K-feldspar grains and c) mica crystal

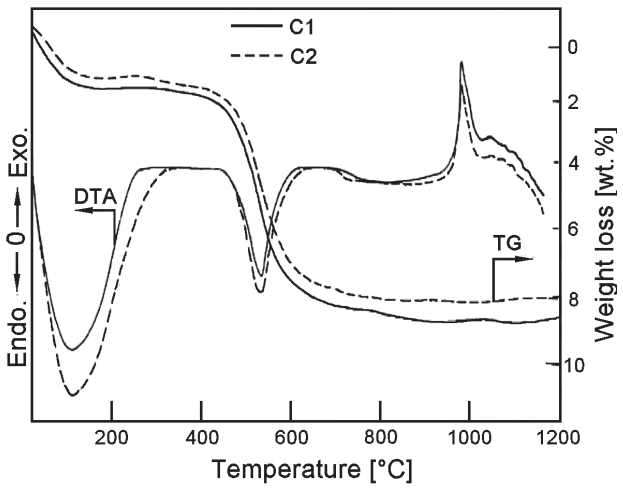

Figure 4. DTA-TGA curve of the investigated samples

Table 4. Mineral composition of Southern Saudi pegmatite (three samples were used for the measurement)

Sample No.	Microcline [wt.%]	Albite [wt.%]	Quartz [wt.%]
1	56.05	17.96	23.28
2	55.52	18.63	23.29
3	57.62	17.70	22.83

Scanning electron microscope (SEM) indicates that the pegmatite samples include some impurities such as magnetite and mica crystals. In addition, the sizes of impurities range from 60 micron to one millimetre. For example, magnetite falls in the range from 60 to 100 μm (Figs. 3a,b) while mica crystals are reaching about 1 mm (Fig. 3c)

Electron microprobe (EMP) shows that the Southern Saudi pegmatite composed of potash feldspar (microcline) as a major mineral phase ranging from 55.05 to 57.62 wt.%. Quartz was found as secondary mineral with 22.83 to 23.29 wt.%, while albite mineral had 17.70 to 18.63 wt.% (Table 4). This method also gives details of chemical composition of each constituent mineral (Table 5).

The raw materials used to prepare the porcelain ceramic bodies play a vital role in ultimate product quality. All the raw materials used in the study were chemically analysed, and the results are given in Table 1. The chemical composition of C1 and C2 bodies is given in Table 2. It may be observed from Table 2 that the C2 body contains comparatively lower amounts of Fe_2O_3 and TiO_2 due to the upgrading process of the Southern Saudi pegmatite used, and this is advantageous for white-based vitrified porcelain as their presence in extra amounts leads to colouration in the fired body [18]. Johnson and Pask [19] also observed that impurities such as Fe_2O_3 and TiO_2 affect the formation kinetics and morphology of mullite.

DTA-TGA curves for both C1 and C2 are presented in Fig. 4. The DTA-TGA curve indicates endothermic peaks at 113 °C due to the removal of physically adsorbed water followed by de-hydroxylation of kaolin (clay) initiated at almost similar temperatures (536 °C) for both C1 and C2, and by this process kaolin transforms to metakaolin [20–22]. The nature of the peak further indicates that dehydroxylation is an endothermic process. These measurements are very important in optimising fast-fired ceramic bodies' profiles.

The plot of linear dilatation with temperature (Fig. 5) indicates the densification behaviour of compact green samples of C1 and C2 compositions with temperature. This test is conducted at a constant heating rate (10 ºC/min) up to 1200 °C. The initial increase in length is observed due to the thermal expansion of the material. Then distinct changes in the curves are seen

Table 5. Chemical analysis of the mineral constituents of the studied pegmatite samples

Oxides	Microcline [wt.%]	Quartz [wt.%]	Albite [wt.%]	Magnetite [wt.%]
SiO_2	64.78	99.93	68.72	24.71
TiO_2	0.00	0.00	0.01	0.00
Al_2O_3	18.38	0.00	19.42	8.39
Cr_2O_3	0.00	0.00	0.02	0.00
FeO	0.01	0.01	0.01	57.81
MnO	0.00	0.00	0.00	0.02
MgO	0.00	0.00	0.00	0.01
CaO	0.01	0.00	0.14	0.14
Na_2O	2.86	0.01	11.71	6.31
K_2O	12.86	0.03	0.06	0.05
Total	98.90	100.01	100.11	97.43

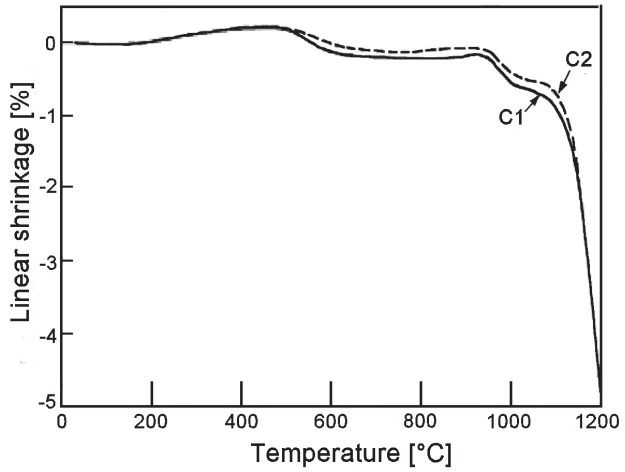

Figure 5. Percentage linear dilatation of the investigated samples with temperature

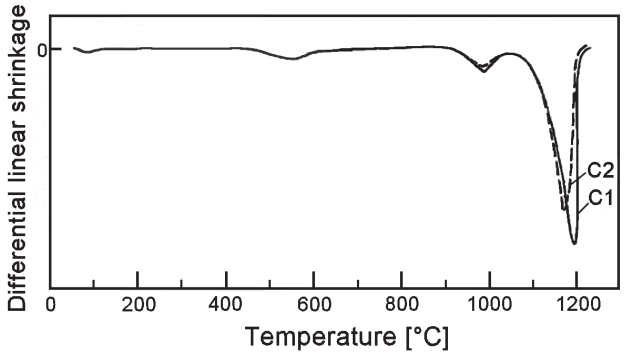

Figure 6. Differential shrinkage plot of the investigated samples

Table 6. Peak densification temperature (PDT), bulk density (BD) and percent of water absorption (WA%) of the samples densified in the dilatometer

Sample	PDT [°C]	BD [g/cm^3]	WA%
C1	1171	2.39	0.45
C2	1195	2.41	0.27

at around 530 °C when kaolin transforms to metakaolin by the dehydroxylation process. After removal of lattice water, the clay matrix starts shrinking, followed by its conversion into a spinel-like structure at around 980 °C. These observations are also supported by the results of DTA-TGA discussed earlier. As the temperature further increases, porosity is eliminated by the viscous flow of glassy phases, which finally results in densification. The differential shrinkage plot indicates the rate of densification achieved at a specific temperature (Fig. 6). Furthermore, in both compositions, a remarkable increase in densification rate is observed at above 1100 °C. A comparison between the two compositions shows that C2 (feldspar after magnetic separation.) undergoes maximum densification at 1195 °C compared to a lower temperature (1171 °C) for C1 (feldspar before magnetic separation).

Porcelain composition containing feldspar after magnetic separation (C2) can be densified at the temperature of 1195 °C, which is 24 °C higher than the temperature required for the porcelain with the feldspar before magnetic separation (C1). The densified samples after the dilatometric study were tested for bulk density and water absorption percentage to verify their degrees of vitrification. The results are given in Table 6. The variation in physico-mechanical properties and colour of the samples fired in an electric furnace at different temperatures is graphically represented in Figs. 7a-e. It can be seen from Fig. 7a that there is no significant difference in shrinkage value between the two compositions C1 and C2. However, as it could be seen from Fig. 7b, bulk density increased with temperature and reached a maximum value at 1200 °C in both cases. The C2 body achieved higher bulk densities at all temperatures. As expected, the ratio of water absorption percentage decreased with increasing heating temperature (Fig. 7c), due to the elimination of pores through liquid phase sintering. The figure also indicates that

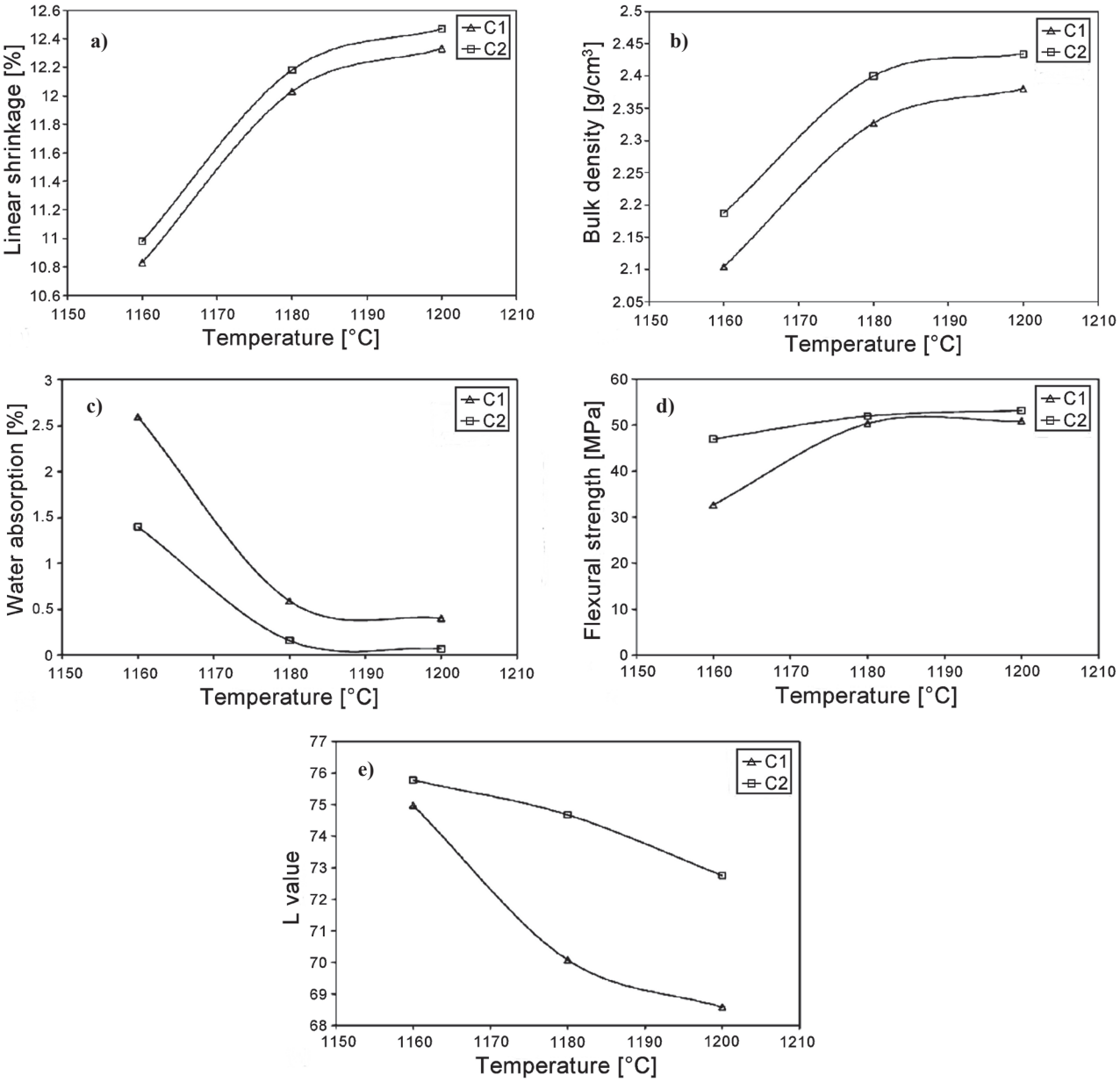

Figure 7. Variation in physico-mechanical properties and *L*-value of C1 and C2 samples with temperature: a) linear shrinkage, b) bulk density, c) water absorption, d) flexural strength and e) *L*-value

C2 achieved water absorption percentage of 0.16 % at 1180 °C compared to 0.59 % at 1200 °C for water absorption of C1. This result also supports the observations made from dilatometric studies (Table 6). Figure 7d shows the flexural strength of the samples fired in the range of 1160–1200 °C.

The flexural strength was found to increase with increasing firing temperature and reached maximum values of around 51 MPa for C1 and 53 MPa for C2 compositions. Increase in flexural strength and bulk density were also observed by other authors for triaxial ceramic compositions [23]. Theoretically, a maximum flexural strength develops in a porcelain body when apparent porosity decreases to zero. A similar trend is observed in the present study also. The resulting vitrified ceramic samples obtained in the present investigation were subjected to colour measurement using the opponent-colour coordinate system developed by Hunter [24]. In this system, the third coordinate describes the lightness of colour and is usually denoted by *L*. The results are graphically represented in Fig. 7e. It may be observed that the *L*-value decreases as the body approaches vitrification at higher temperatures. This is probably due to the increased intensity of colour-forming oxides Fe_2O_3 and TiO_2 present in the raw materials at higher temperatures. It may also be noted that the composition containing pegmatite after magnetic separation containing composition (C2) showed a higher *L*-value (whiter) due to the presence of lower amounts of Fe_2O_3 and TiO_2, compared to the composition containing feldspar before magnetic separation containing composition (C1).

IV. Conclusions

The sequence of chemical reactions in the studied porcelain compositions followed similar reaction steps up to 1000 °C, beyond which feldspar forms an eutectic melt and starts reacting. The porcelain composition containing pegmatite after magnetic separation exhibits a maximum densification rate at 1195 °C compared to 1171 ºC of pegmatite- containing composition before magnetic separation. The treated pegmatite lead to higher bulk density (2.43 g/cm^3), a lower percentage of water absorption (0.07 %), and highest flexural strength (53.14 MPa) at 1200 °C compared to untreated pegmatite.

The whiteness of the porcelain ceramic bodies produced by the treated pegmatite is of better values than those obtained using untreated pegmatite in which Fe_2O_3 and TiO_2 impurities are present. The present study provides positive indications for usage of Southern Saudi pegmatite after treatment in ceramic industries.

Acknowledgements: The authors are greatly indebted to Dr. A. El-Maghraby Department of Chemistry, Faculty of Science, Taif University, Saudi Arabia for his assistance.

References

1. P.W. Harben, p. 306 in *The Industrial Minerals Handbook*, 3rd ed. Industrial Minerals Information Services Ltd., Worcester Park, UK, 1999.
2. P.W. Harben, p. 412 in *The Industrial Mineral Handbook: A guide to markets, specification and prices*. 4th ed. Industrial Minerals Information, Worcester Park, UK, 2002.
3. C.W. Sinton, p. 368 in *Raw Materials for Glass and Ceramics: Sources, Processing, and Quality Control*, John Wiley & Sons, Inc., New York, 2006.
4. C.M.F. Vieira, T.M. Soares, R. Sanchez, S.N. Monteiro, "Incorporation of granite waste in red ceramics", *Mater. Sci. Eng. A*, **373** [1–2] (2004) 115–121.
5. W.D. Kingery, H.K. Bowen, D.R. Uhlmann, *Introduction to Ceramics*, 2nd ed. Wiley, New York, 1976.
6. G.P. Emiliani, F. Corbara, p. 197, *Tecnolog'ia Ceramica-La Lavorazione*, Gruppo Editoriale, Faenza Editrice, Faenza, Italy, 1999.
7. Ch. Schmidt-Reinholz, H. Schmidt, "On the effect of feldspar in brick bodies and products [Ueber die Wirkung von Feldspat in Ziegelmassen und-Erzeugnissen]", *Keramische Zeitschrift*, **47** [8] (1995) 607–612.
8. J.F. Schairer, N.L. Bowen, "Melting relation in the system $Na_2O{\cdot}Al_2O_3{\cdot}SiO_2$ and $K_2O{\cdot}Al_2O_3{\cdot}SiO_2$", *Am. J. Sci.*, **245** (1947) 193–204.
9. W.E. Lee, W.M. Rainforth, p. 604 in *Ceramic Microstructures Property Control by Processing*. Chapman & Hall, London, UK, 1994.
10. M.W. Carty, U. Senapati, "Porcelain-raw materials, processing, phase evolution and mechanical behaviour", *J. Am. Ceram. Soc.*, **81** (1998) 3–20.
11. Y. Iqbal, W.E. Lee, "Fired porcelain microstructures revisited", *J. Am. Ceram. Soc.*, **82** (1999) 3584–3590.
12. Y. Iqbal, W.E. Lee, "Microstructural evolution of porcelain", *J. Am. Ceram. Soc.*, **83** (2000) 3121–3127.
13. H.B. Johnson, F. Kessler, "Kaolinite dehydroxylation kinetics", *J. Am. Ceram. Soc.*, **52** (1969) 199–204.
14. K. Okada, N. Otsusa, "Characterization of the spinal phase from SiO_2-Al_2O_3 xerogels and the formation process of mullite", *J. Am. Ceram. Soc*., **69** (1986) 652–656.
15. B. Sonuparlak, M. Sarkiaya, L.A. Aksay, "Spinel phase formation during 980 °C exothermic reaction in the kaolinite-to-mullite reaction series", *J. Am. Ceram. Soc.*, **70** (1987) 837–842.
16. K.H. Schuller, "Reaction between mullite and glassy phase in porcelain", *Trans. Br. Ceram. Soc.*, **63** (1964) 102–117.
17. W.A. Deer, R.A. Howie, J. Zussman, p. 696 in *Rock-Forming Minerals*, 2nd ed. Longman Scientific and Technical, London, 1992.
18. S. Kumar, K.K. Singh, P. Ramachandrarao, "Effect of fly ash additions on the mechanical and other properties of porcelainised stoneware tiles", *J. Mater. Sci.*, **36** (2001) 5917–5922.
19. S.M. Johnson, J.A. Pask, "Role of impurities on formation of mullite from kaolinite and Al_2O_3-SiO_2 mixtures", *Am. Ceram. Soc. Bull*., **61** (1982) 838–842.
20. G.W. Brindley, J. Nakahira, "The kaolinite-mullite reaction series", *J. Am. Ceram. Soc*., **42** [7] (1959) 311–319.
21. G.W. Brindley, J. Nakahira, "The kinetics of dehydroxylation of daolinite and halloysite", *J. Am. Ceram. Soc.*, **40** [10] (1957) 346–350.
22. K.J.D. Mackenzie, I.W. Brown, R.H. Meinhold, M.E. Browden, "Outstanding problems in the kaolinite-mullite reaction series investigated by ^{29}Si ^{27}Al solid state nucler magnetic resonance: I metakaolinite", *J. Am. Ceram. Soc*., **68** [6] (1985) 293–298.
23. O.I. Lee, Z. Nakagawa, "Bending strength of porclaine", *Ceram. Int.*, **28** (2002) 131–140.
24. R.S. Hunter, "Photoelectric tristimulus colorimetry with three filters", *J. Opt. Soc. Am.*, **32** (1942) 509–538.